W. ŻÓRAWSKI*, M. MAKRENEK**, A. GÓRAL***,#

MECHANICAL PROPERTIES AND CORROSION RESISTANCE OF HVOF SPRAYED COATINGS USING NANOSTRUCTURED CARBIDE POWDERS

Nanostructured and composite WC-12Co coatings were prepared by means of the supersonic spray process (HVOF). The microstructure and composition of WC-12Co nanostructured powder were analyzed by scanning electron microscope (SEM) and transmission electron microscope (TEM). Investigations revealed nano grains of WC with the size in the range of 50-500 nm. The nanostructured sprayed coating was analysed by SEM and phase composition was investigated by X-ray diffractometer (XRD). A denser coating structure with higher hardness was observed compared to conventional coating with a small amount of W_2C, WC_{1-x}, W and some amorphous phase. Young's modulus and hardness were determined by depth sensing indentation in HVOF sprayed WC-12Co nanostructured coatings. Results were compared to conventional coatings and the relevance of the nanostructure was analyzed. An indentation size effect was observed on the polished surface and cross-section of both coatings. Data provided by indentation tests at maximum load allow to estimate hardness and elastic modulus. Enhanced nanomechanical properties of conventional coating in comparison to nanostructured one were observed. Nanostructured coatings WC-12Co (N) revealed significantly better corrosion resistance.

Keywords: WC-12Co, HVOF, mechanical properties

1. Introduction

Nanostructured materials provide new possibilities, which enable creating composite structures with much better properties than composites obtained from conventional materials. Tungsten carbide is the material used for numerous applications. Taking its high level of hardness into consideration, it is most often used material in the form of sinter with cobalt, which guarantees its high durability. Its outstanding wear resistance contributed to the use of WC-Co to increase durability of various machine parts [1,2]. The structure of the sprayed coatings is composed of hard WC grains deposited in a cobalt matrix. Today HVOF spraying is currently used for WC-Co application because atmospheric plasma spraying (APS) with higher temperature of the process leads to its decomposition, decarburization and oxidation what significantly decreases properties of coatings. Higher velocity and lower temperature of HVOF process allow to form very dense coatings with larger fraction of retained WC and excellent adhesion to the substrate [3-6].

Mechanical characterization of thermally sprayed coatings is complex task because of theirs heteregenous microstructure and inherent porosity. Standard methods usually do not enclose this problem. Nanoidentation allows to obtain reliable properties taking into account the size effect of microstructure components [7-9].

In the present paper, WC–12Co nanostructured and conventional coatings were prepared by means of liquid-fuel HVOF spraying technology to investigate the microstructure, nanomechanical properties and corrosion resistance of the deposited coatings.

2. Experiment

Nanostructured WC-12Co, with a granularity of -45 + 5µm (Infralloy S7412) and conventional WC-12Co (Amperit 519.074), with a granularity of -45 + 5.5 µm were HVOF sprayed. The nanostructured powder and coating were denoted as WC-12Co (N), the conventional materials were denoted as WC-12Co (A). The coatings were deposited by means of TAFA JP-5000 system with kerosene as a fuel with spraying parameters: an oxygen flow rate – 890 l/min, a kerosene flow rate – 22.7 l/min, a barrel length – 150 mm, a spray distance – 380 mm.

The structure and chemical composition of the powders and the coatings were analyzed using the following scanning microscopes: JSM–5400 with an ISIS 300 Oxford (EDS) microprobe and FEI Nova™ NanoSEM 200. The SEM and TEM analysis was the base to evaluate crystal size grains in nanostructured powder and coating. Their phase composition was studied using a Bruker D8 Discover diffractometer with Co-Kα radiation of wavelength λ = 1.78897 Å. An Nanovea nanoindenter was applied to analyse the nanohardness and Young's modulus of the resultant polished coating with a calibrated Berkovich indenter. The reference material for

* KIELCE UNIVERSITY OF TECHNOLOGY, FACULTY OF MECHATRONICS AND MACHINE BUILDING, POLAND
** KIELCE UNIVERSITY OF TECHNOLOGY, FACULTY OF MANAGEMENT AND COMPUTER MODELLING, POLAND
*** INSTITUTE OF METALLURGY AND MATERIALS SCIENCE POLISH ACADEMY OF SCIENCES, 25 REYMONTA , 30-059 KRAKOW, POLAND
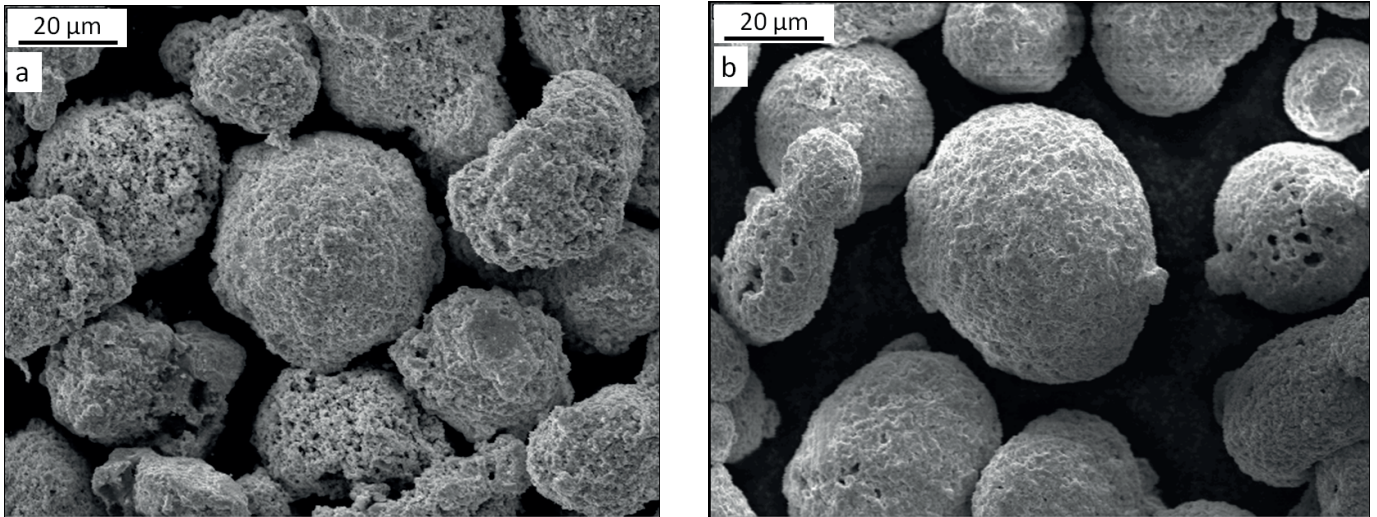# Corresponding author: a.goral@imim.pl

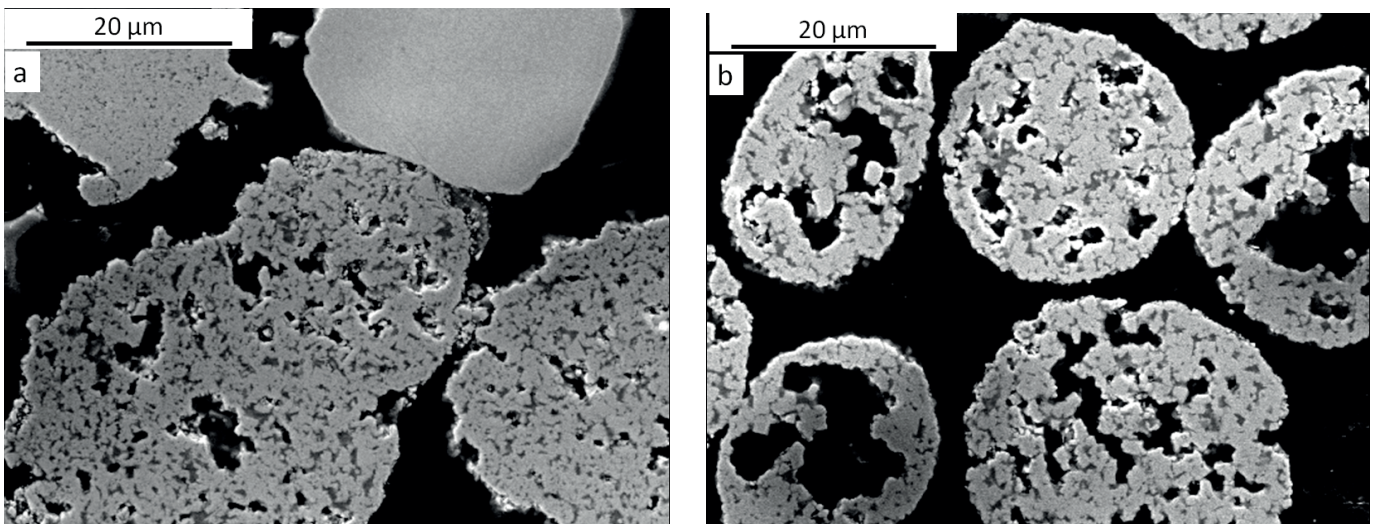Fig. 1. Powder grains: a) WC-12Co (N), b) WC-12Co (A)

Fig. 2. Cross-section of powder grains: a) WC-12Co (N), b) WC-12Co (A)

nanointender calibration was sample of silica. The indentations were performed at constant depth 0.1 µm. The corrosion resistance of "as sprayed" samples were carried out by means of device Atlas'99 (Atlas-Solich).

The samples for indentation were prepared in plan view and cross-section from the as sprayed coatings. The topography of the coatings after polishing was analyzed by means of a Talysurf CCI-Lite non-contact 3D profiler [10,11].

3. Results and discussion

3.1. Microstructure and phase composition

The shape and cross-section of powder grains of both sprayed powders are shown in Figs. 1 and 2, respectively. They are manufactured by agglomeration and sintering of fine powder grains. For nanostructured powder nanometric and submicron WC crystals in the range of 50-500 nm (Fig. 3) were applied. Conventional WC-12Co (A) powder consists of 1 µm grains. High internal porosity of both powders is well seen (Fig. 2).
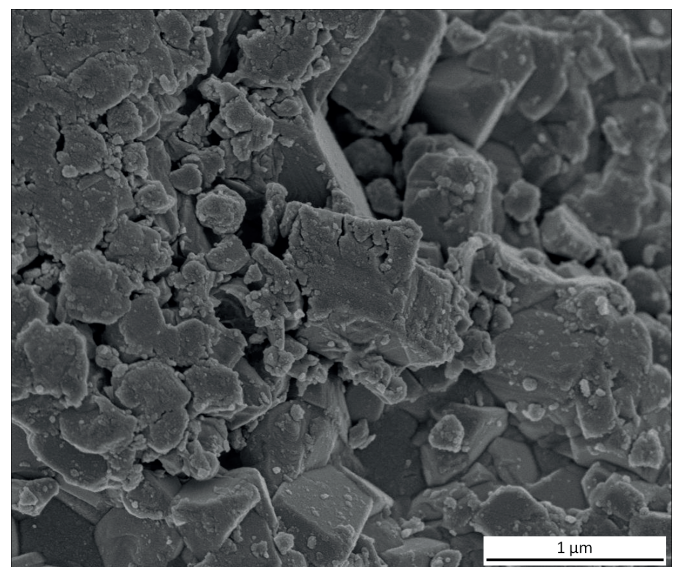

Fig. 3. Nanometer and submicron WC-12Co (N) powder particles on the cross section of powder grain

The microstructures of both HVOF sprayed coatings are presented in Fig. 4. Metallographic images of the two WC-12Co coatings showed that there were some small undeformed tungsten carbide grains embedded in the cobalt matrix (Fig.5). From the EDS microanalysis, it was clear that the coating content was different in each zone. The light-coloured grains in the WC-12Co coatings confirm a high amount of tungsten, whilst the dark-coloured matrix is an area with a high content of cobalt and a low content of tungsten. Different sizes of tungsten carbide grains were visible in both coatings.

The coating deposited using the nanostructured powder had a finer-grained structure with unmodified nanocrystals. It exhibited lower porosity, despite the fact that the nanostructured powder contained larger grains. The coating produced from the conventional powder, on the other hand, had higher porosity, resulting from the higher porosity of the grains, which can be seen in the metallographic images.

Microstructure in bright field (BF) TEM and related electron diffractions from an area with grains of different Co content are shown in Fig. 6. In the area with enhanced Co content, an amorphous structure occurs, and crystallite grains possess a hexagonal WC structure. The dimensions of WC grains are in the range of 200-500 nm.

Analysis of the powder diffraction patterns showed that the WC grains in the nanostructured powder were half the size of those in the conventional powder. The diffraction patterns revealed the presence of WC and Co both in the WC-12Co powder and in the deposited coating (Figs. 7 and 8). The new phases that appeared in both coatings, i.e. W_2C, WC_{1-x} and W, were attributable to the prior disintegration of WC in the spray stream. The diffraction lines of the phases after spraying were considerably wider. This testified to a significant degree of elastic and plastic deformation, i.e. a high level of energy stored in the form of network defects; this particularly in the case of the Co phase [6].
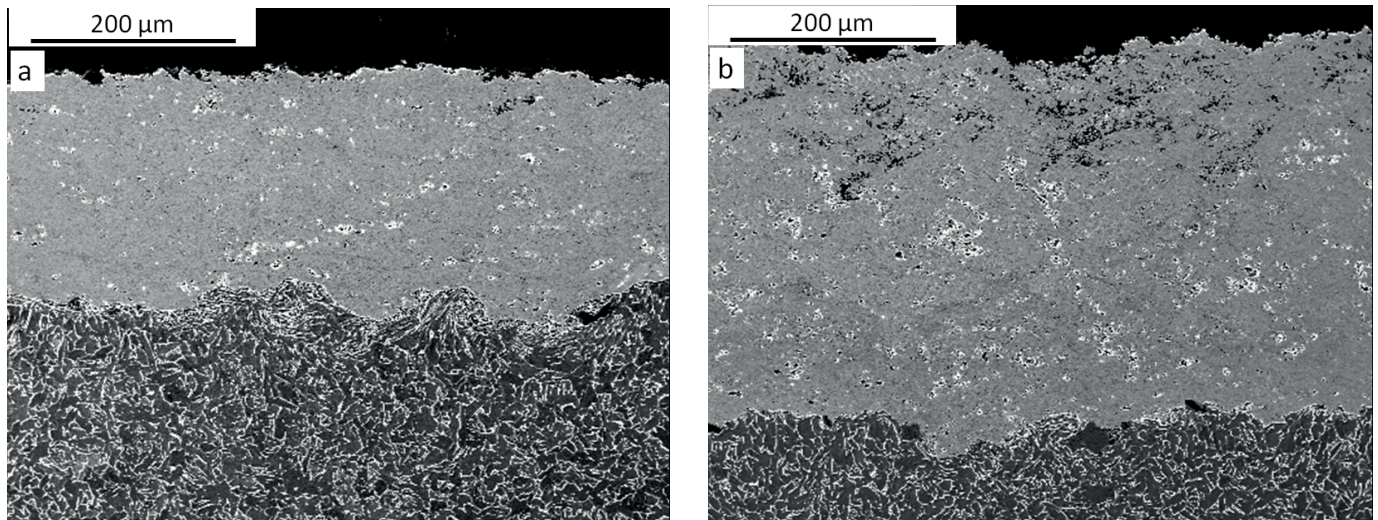

Fig. 4. Cross-section of HVOF sprayed coatings: a) WC-12Co (N) 200x, b) WC-12Co (A) 200x
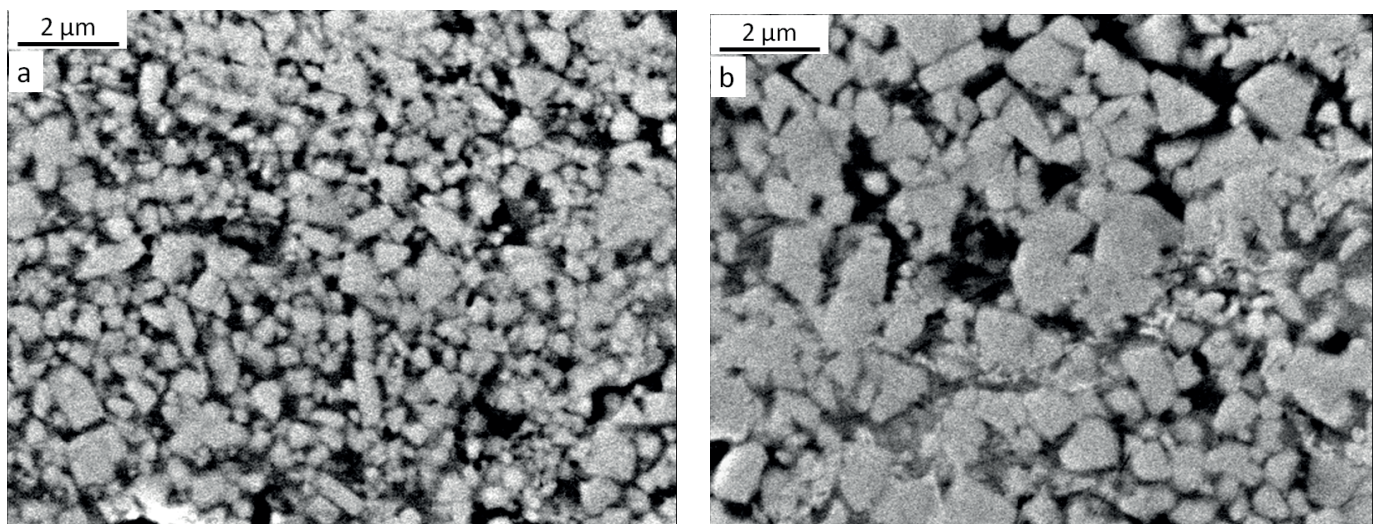

Fig. 5. Cross-section of HVOF sprayed coatings: a) WC-12Co (N) 5000x, b) WC-12Co (A) 5000x
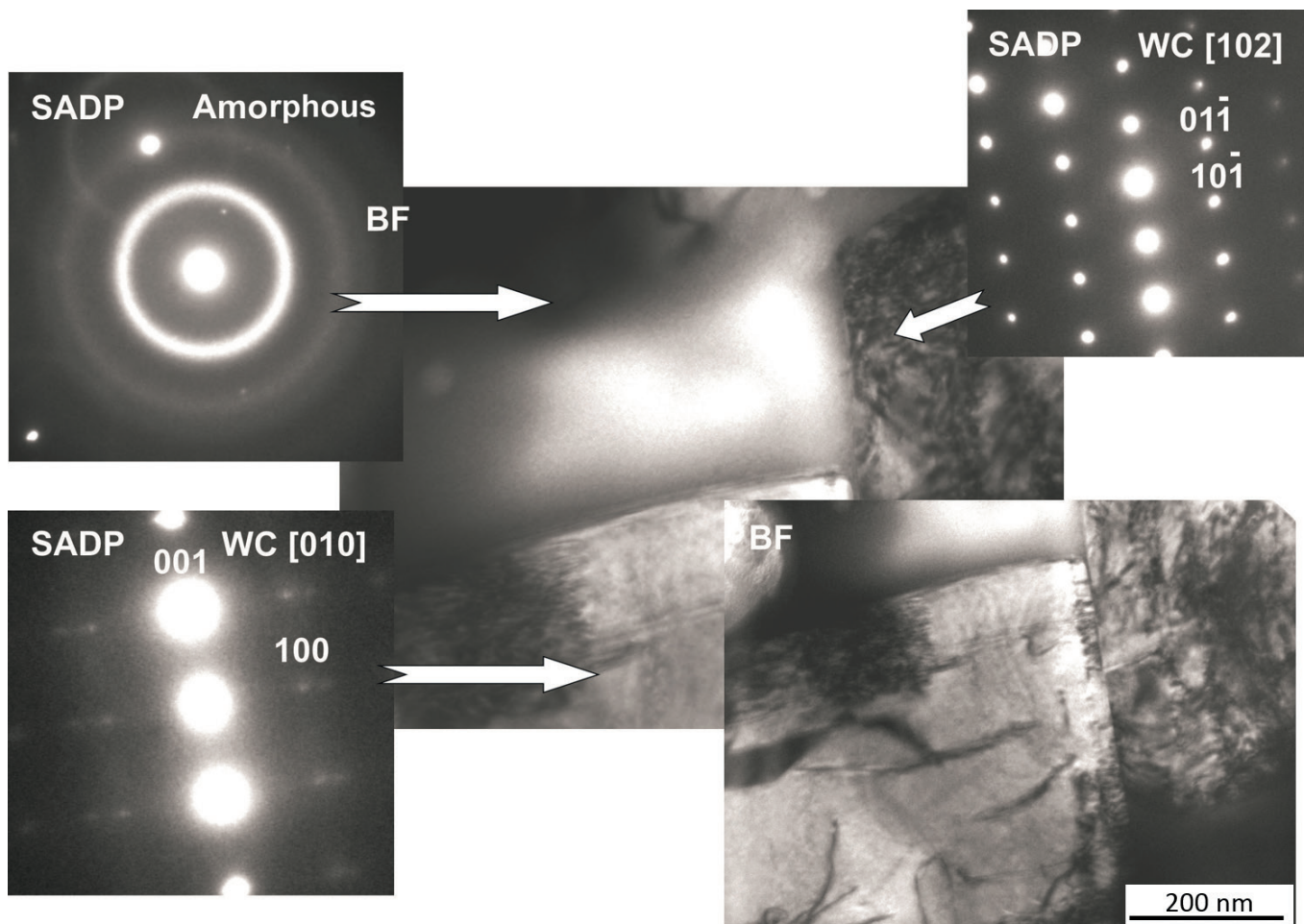
Fig. 6. TEM microstructure of HVOF sprayed WC-12Co (N) coating

Analysis of WC-12Co Amperit and WC-12Co Nanox showed that they are composed of WC and Co and they do not have any other phases. Analysis of WC-12Co Amperit (Fig. 8) and WC-12Co Nanox coatings proved the presence of WC and Co, which were also present in both WC-12Co powders as well as new phases, namely: W_2C, WC_{1-x} and W, which result from decomposing WC which, in turn, is a consequence of the spraying stream affecting powder grains. W and C present in the grains of nanopowder reacted forming new WC and W_2C phases, whilst cobalt reacted with tungsten and carbon forming Co_3W_3C (η-carbide); $W+C\rightarrow WC$, $2W+C\rightarrow W_2C$, $3W+3Co+C\rightarrow Co_3W_3C$. Co_3W_3C occurs mainly during sintering at 800 °C as a result of coercive force. Furthermore, Co_6W_6C carbide is formed at this temperature and the following reactions take place; $2W+C\rightarrow W_2C$, $2Co_3W_3C+W\rightarrow Co_6W_6C+WC$, $Co_3W_3C+2C\rightarrow 3WC+3Co$ [12,13].

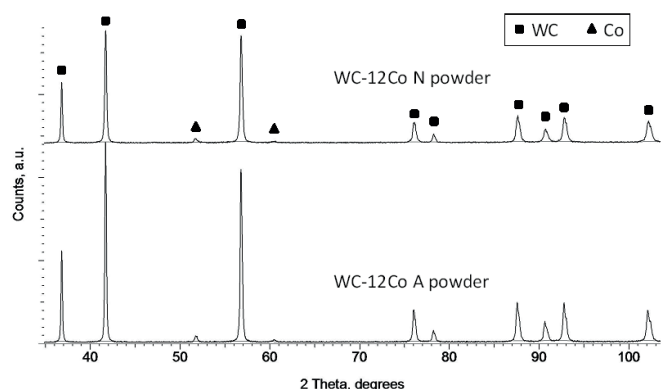

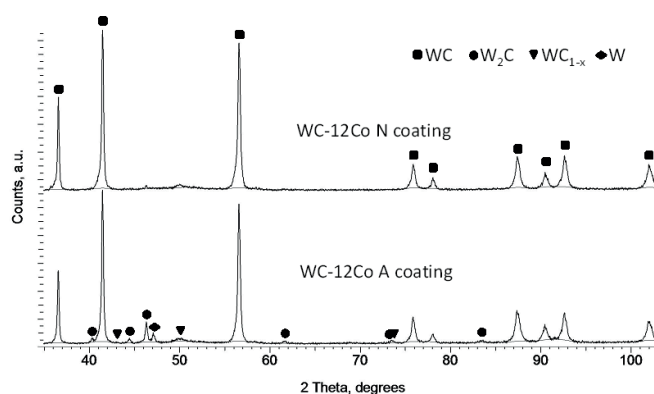Fig. 7. XRD patterns of WC-12Co (N) and WC-12Co (A) powders

Fig. 8. XRD patterns of HVOF sprayed WC-12Co (N) and WC-12Co (A) coatings

3.2. Surface topography of coatings

Surface topography, depth histogram and bearing curve for both coatings are presented in Figs. 9 and 10. The slight slope of bearing curve reflected the mirror surface of samples after polishing. Measurements of topography of sprayed coatings showed that the arithmetic mean of the surface height S_a of the WC–12Co (N) coating was very low but slightly higher than for the conventional coating (6.743 nm and 5.728 nm, respectively). Moreover the other surface topography of both sprayed coating were nearly the same (Tab. 1).

TABLE 1

Surface topography parameters according to ISO 25178

Parameter	Surface after polishing	
	WC-12Co (N)	WC12-Co (A)
Sa,	6.743 nm	5.728 nm
Sq,	9.75 nm	8.87 nm
Ssk	-0.77	-1.38
Sku	7.05	9.99
Sp,	39.55 nm	37.95 nm
Sv,	34.67 nm	36.27 nm
Sz,	74.22 nm	74.22 nm

The skewness parameter S_{sk} was negative what indicate on concentration of material nearby of profile top, testified topography plateau. The high value of kurtosis S_{ku} is result of presence of grooves in the profile of surface which are remnants of coatings porosity. The other topography parameters as the maximum peak height S_p, the maximum pit height S_v and maximum height are in nanometric dimension what confirm flatness of sample surfaces. It can be concluded that topography of sprayed coatings after polishing do not depend on the microstructure of applied powders.

3.3. Nanoindentation of coatings

The hardness and Young's modulus of the investigated microstructures were analysed using a square grid for nanoindentation tests on the polished samples in plan view from the as-sprayed coatings and on the cross-sections of coatings (Tab. 2). The distance between each nanoindentation
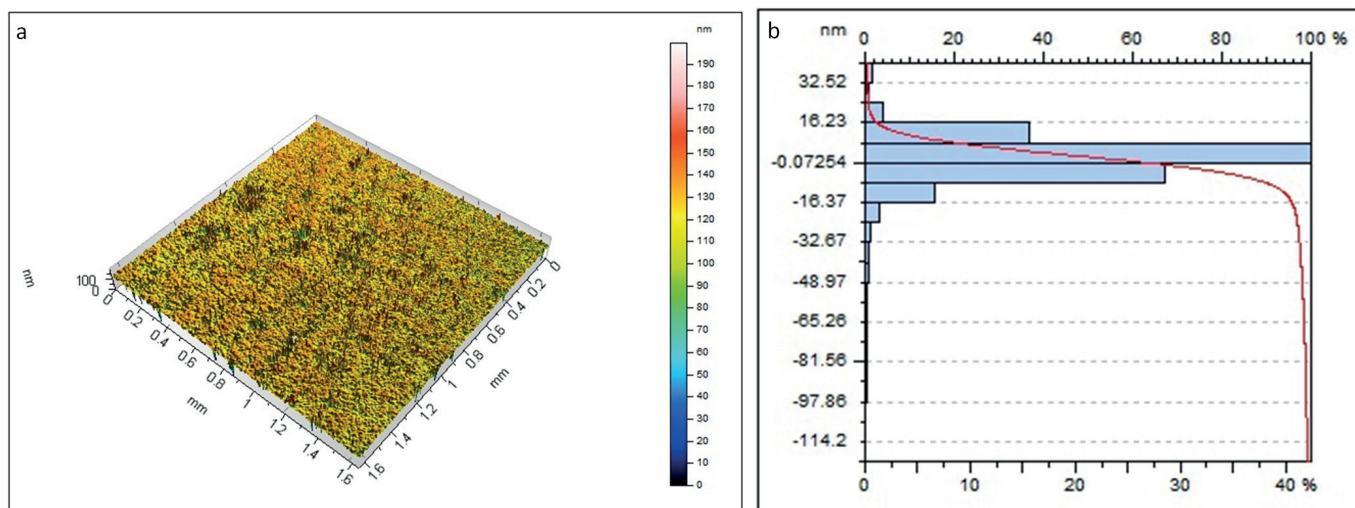

Fig. 9. WC-12Co (N) coating: a) surface topography, b) depth histogram and bearing curve
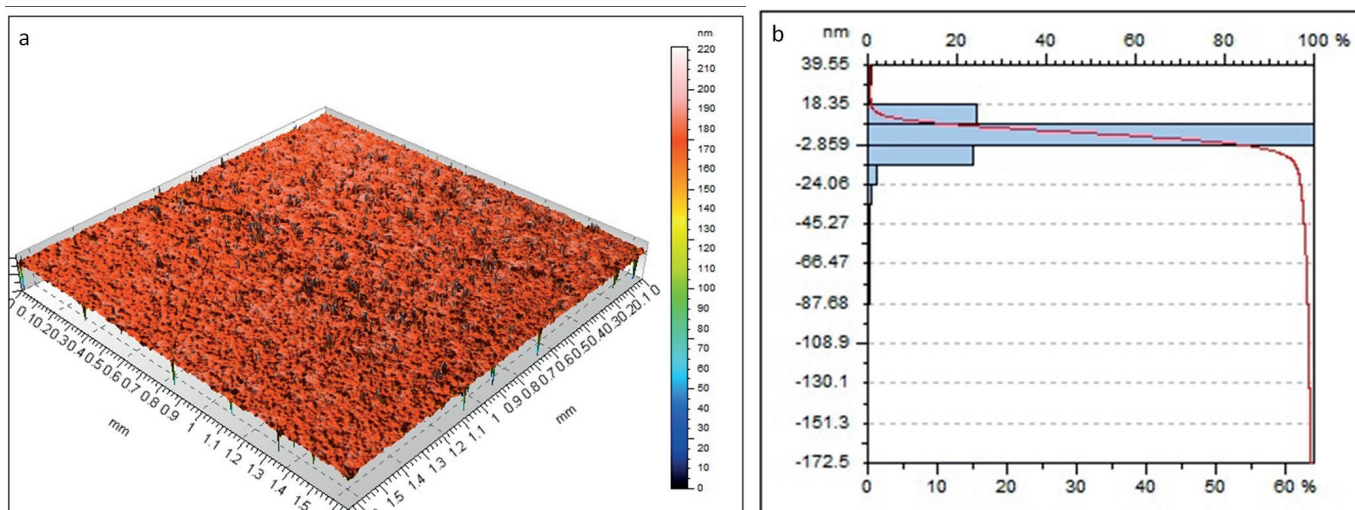

Fig. 10. WC-12Co (A) coating: a) surface topography, b) depth histogram and bearing curve
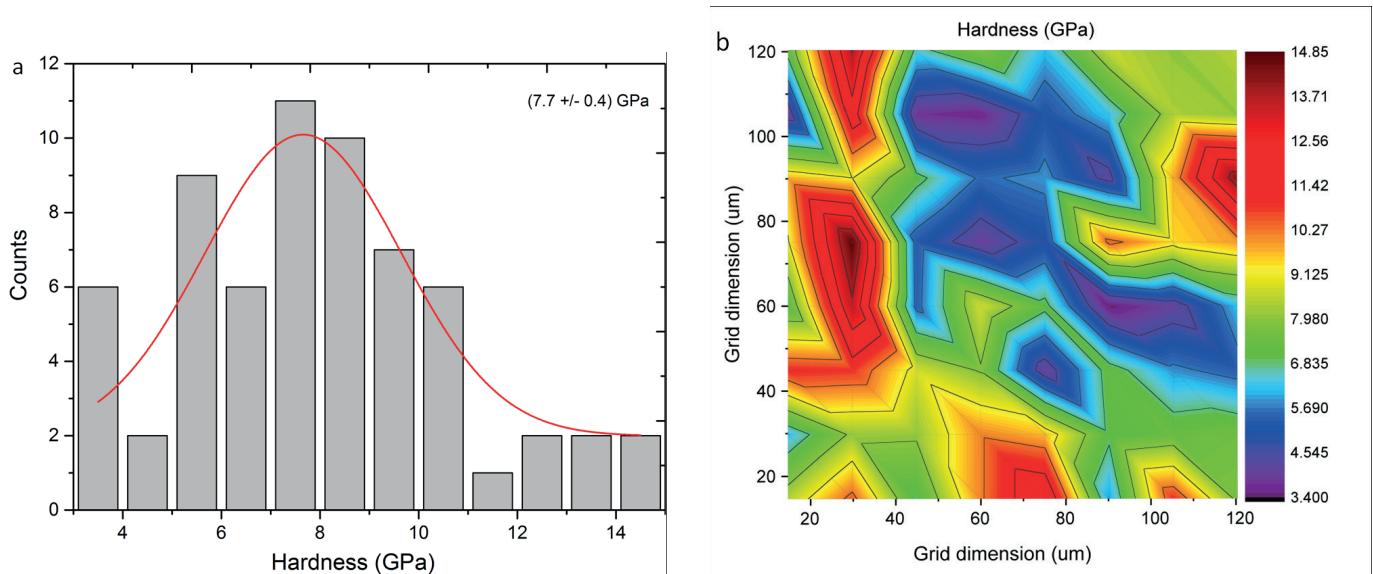
Fig. 11. Distribution of WC-12Co (N) coating hardness: a) histograms and probability, b) map
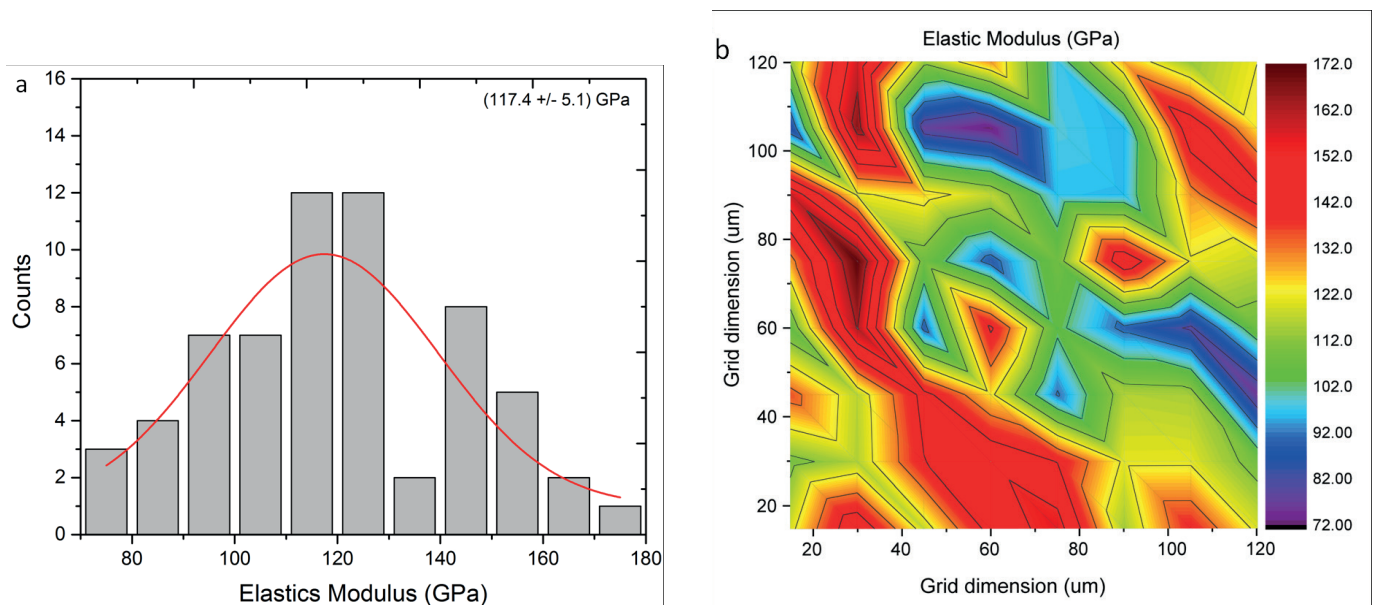

Fig. 12. Distribution of WC-12Co (N) coating Young's modulus: a) histograms and probability, b) map

was changed by nanointender as 1 μm. The distributions of the nanomechanical properties were as then plotted as histogram distributions and maps of surface in which each hardness and Young's modulus result was showed on the charts with the same dimensions and locations as in the investigated areas. Histograms and probability distributions of the hardness and Young's modulus on the cross-section of WC-12Co (N) coating is shown in Figs. 11 and 12, respectively.

Nanoindentation tests showed a distribution of the mechanical properties (hardness and Young's modulus) which is related to the different areas (molten and partially molten) present in the coatings. However, the main constituents of both coatings are tungsten carbide grains embedded in the cobalt matrix, the additional phases created after supersonic spraying (W_2C, WC) and inherent porosity revealed high scattering of results (Figs. 11 and 12).

Obtained results are the mean values from all phases existing in the tested area because individual hardness and elastic modulus of each phase are very difficult to measure. Nanohardness of the WC-12Co (A) sample point to the dominant value of 10.8 GPa, which is the highest value of all measured places. Hardness measured onto the polished surface of coatings showed higher values than in the cross-section of coating. Additional finishing processes of the surface as grinding, polishing and lapping probably caused reinforcement of coating matrix and increase of coating

TABLE 2

The hardness and Young's modulus of WC-12Co coatings

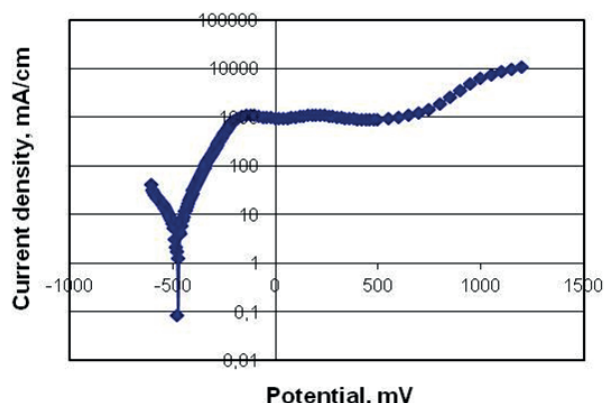| Coating/place of measurement	Hardness (GPa)	Elastic modlulus (GPa)
WC-12Co (N) /surface	9.9 ± 0.3	196.9 ± 9.4
WC-12Co (N) /cross-section	7.7 ± 0.4	117.4 ± 5.1
WC-12Co (A) /surface	10.8 ± 0.6	257.8 ± 13.6
WC-12Co (A) /cross-section	6.9 ± 0,5	177.9±16.7

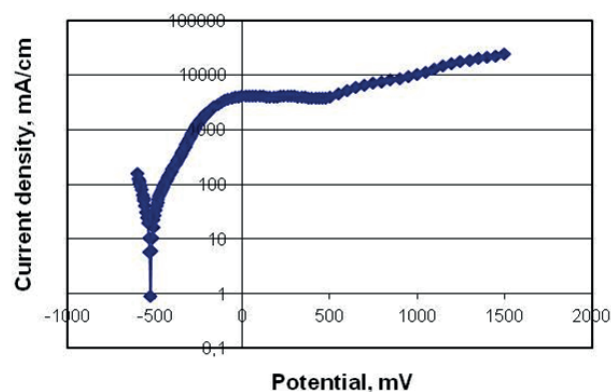Fig. 13. Polarization curve for WC-12Co (N) coating

Fig. 14. Polarization curve for WC-12Co (A) coating

surface hardness. In both cases WC-12Co (A) revealed higher Young's modulus than for WC-12Co (N) coating. Significant differences may be attributed to the differences in tungsten carbide grains in the both coatings [14]. The presence of nanostructured grains of WC in the coating cause decrease its mechanical properties.

3.4. Corrosion resistance

Corrosion resistance of HVOF carbide coatings is important factor determining possibility of applications in different environments [17-19]. Potentiodynamic polarization corrosion method was applied to evaluate HVOLF sprayed WC-12Co coatings. Anodic and cathodic curves were obtain by polarization of both samples with the rate of potential change of at 0.2 mV/s (in the area ± 200 mV from corrosion potential) and 0.4 mV/s in the area of higher potentials. Samples with the singled area 10 mm diameter were polarised to 500 mV potential. Polarization curves were received after 24 hours of exposition in the test solution (3,5% NaCl) in order to determine corrosion potential (Figs. 13 and 14). Tests were carried out at room temperature -21 °C ± 1 °C. Results of experiments are parented in Table 3. Based on obtained results it can be conclude that supersonic sprayed nanostructured coatings WC-12Co (N) depicted significantly better corrosion resistance in comparison to conventional coating. Both, density of corrosion current and corrosion potential were significantly lower for nanostructured coating. The reason of different corrosion resistance were differences in coatings microstructure, phase composition and porosity [15,16].

4. Conclusions

New phases W_2C and W_{1-x} appeared in the supersonic sprayed WC-12Co coatings.

Parameters of topography of both sprayed WC-12Co coatings after polishing do not depend on the microstructure of applied powders.

The highest hardness and Young's modulus revealed the conventional coating WC-12Co (A) onto the surface of coating.

HVOF sprayed nanostructured coatings WC-12Co (N) present significantly better corrosion resistance in comparison to the conventional coating.

REFERENCES

[1]   L. Pawlowski: The science and engineering of thermal spray coatings, 2008 J.Willey & Sons Ltd, Chichester, II ed.

[2]   W. Tillmann, P. Hollingsworth, I. Baumann, L. Hiegemann, C. Weddeling, A. E. Tekkaya, S. Rausch, D. Biermann, Surf. Coat. Technol. **268**, 134-141 (2015).

[3]   [A. Lekatou, D. Sioulas, A.E. Karantzalis, D. Grimanelis, Surf. Coat. Technol. **276**, 539-556 (2015).

[4]   S. Al-Mutairi, M.S.J. Hashmi, B.S. Yilbas, J. Stokes, Surf. Coat. Technol. **264**, 175-186 (2015).

[5]   C.-J. Li, G.-J. Yang, Int. J. Refract. Met. H. 39, 2-17 (2013).

[6]   W. Żórawski, Surf. Coat. Technol. **220**, 282-289 (2013).

[7]   J. Rodriguez, A. Rico, E. Otero, W.M. Rainforth, Acta Mater. **57**, 3148-3156 (2009).

[8]   J. Nohava, R. Mušálek, J. Matějíček, M. Vilémová, Surf. Coat. Technol. **240**, 243-249 (2014).

[9]   W. Żórawski, A. Góral, O. Bokuvka, L. Lityńska-Dobrzyńska, K. Berent, Surf. Coat. Technol. **268**, 190-197 (2015).

[10]   S. Adamczak, D. Janecki, K. Stępień, Measurement **44** (1) 164-173 (2011).

[11]   D. Janecki., Stepień K., Adamczak S., Measurement, **43**, 659-663 (2010).

[12]   Handbook of Thermal Spray Technology, J.R. Davis, Davis & Associates, 2004 ASM International.

[13]   C. Bartuli, T. Valente, F. Cipri, E. Bemporad, M. Tului, J. Therm. Spray Technol. **14**, 187-195 (2005).

[14]   P. Chivavibul, M. Watanabe, S. Kuroda, C. Shinoda, Surf.

TABLE 3

Corrosion properties of WC-12Co coatings

Coating	Density of corrosion current I_k (µA/cm²)	Corrosion potential E_{CORR}
WC-12Co (N)	6	475
WC-12Co (A)	23,5	525

1846

Coat. Technol. **202** (3) 509-521 (2007).

[15] J.M. Guilemany, S. Dosta, J.R. Miguel, Surf. Coat. Technol. **201**, 1180-1190 (2006).

[16] A. Lekatou, D. Sioulas, A.E. Karantzalis, D. Grimanelis, Surf. Coat. Technol. **276**, 539-556 (2015).

[17] Josep A. Picas, Elisa Rupérez, Miquel Punset, Antonio Forn,

Surf. Coat. Technol. **225** (25) 47-57 (2013).

[18] A. Lekatou, D. Zois, D. Grimanelis. Thin Solid Films, **516** (16) 5700-5705 (2008).

[19] M. Magnani, P.H. Suegama, N. Espallargas, S. Dosta, C.S. Fugivara, J.M. Guilemany, A.V. Benedetti, Surf. Coat. Technol. **202** (19) 4746-4757 (2008).